A theoretical exploration of TypeI/TypeII dual photoreactivity of new promising Ru(II)-dyads for PDT approach

M.E.Alberto,*[a] J. Pirillo,[b] N.Russo,[b] C. Adamo [a,c]

[a] *Chimie ParisTech, PSL Research University, CNRS, Institut de Recherche de Chimie Paris (IRCP), F-75005 Paris, France. E-mail: marta.alberto@chimie-paristech.fr*

[b] *Dipartimento di Chimica e Tecnologie Chimiche, Università della Calabria, Via P. Bucci, 87036 Rende, Italy*

[c] *Institut Universitaire de France, 103 Boulevard Saint Michel, F-75005 Paris, France*

ABSTRACT

Ru(II)-dyads are a class of bioactive molecules of interest as anticancer agents obtained incorporating an organic chromophore in the light-absorbing metallic scaffold. A careful DFT and TDDFT investigation of the photophysical properties of a series of Ru(II)-polypiridyl dyads containing polythiophene chains of different lengths bound to a coordinating imidazo[4,5-f][1,10]phenantroline ligand, is herein reported. The modulation of the crucial chemical and

physical properties of the photosensitizer with the increasing number of thiophene units, has been accurately described investigating the UV-Vis spectra, Type I and Type II photoreactions, also including spin orbit coupling values (SOC). Results show that the low-lying ^{3}IL states afforded as the number of the thiophene ligands increases (n=3,4) are energetically high enough to ensure the singlet oxygen production and can be also involved in electron transfer reaction, showing a dual type I/typeII photoreactivity.

1. INTRODUCTION

Due to their appealing physico-chemical properties, Ru(II) compounds have found wide applications in biological and medical field and are now attracting an increasing interest as potential candidates for Photodynamic Therapy (PDT). [1] The latter is a non-invasive medical approach used for the treatment of several skin diseases and more recently, for the treatment of some types of cancer. [2] The so-called photodynamic effect rests on the oxidative damage of biological material by reactive forms of oxygen generated by sensitized reactions. As currently practiced, a photosensitizing agent (PS) is injected intravenously and it is excited from its ground state S_0 to the first excited state S_1 by using light of a specific wavelength. The S_1 state can relax back to the ground state via a radiative process, the singlet–singlet emission called fluorescence, or via non radiative intersystem crossing (ISC) from the singlet to triplet state. The triplet state generated by the radiationless intersystem crossing, can be quenched through two kinds of processes.

In oxygenated environment and under particular conditions, the chromophore in its excited triplet state can transfer its energy to ground-state molecular oxygen ($^3O_2$), undergoing Type-II photoreactions. [2] The interaction between electronically excited triplet sensitizer and ground-state

molecular oxygen ($^3O_2$) usually involves energy transfer to yield chemically highly active singlet oxygen $^1O_2$ which reacts with many biological molecules, including lipids, proteins, and nucleic acids, leading to cancer cell death. Singlet lowest-energy oxygen $^1O_2(^1\Delta_g)$ can be generated provided that the energy difference Δ_{S-T} of the sensitizer exceeds the energy required to promote the O_2 $^3\Sigma_g^- \rightarrow {}^1\Delta_g$ transition (0.98eV). [2,3]

On the other hand, the excited PS can react directly with organic substrates by electron exchange producing radical intermediates that are subsequently scavenged by oxygen, with the formation of the superoxide oxygen radical species $O_2^{\cdot(-)}$ and other highly reactive radicals. Collectively these reactions are classified as Type-I photoreactions. [2,3]

Type-II processes are believed to predominate in the induction of cell damage and their efficiency depends on many factors, among which the triplet state lifetime and the triplet quantum yield (Φ_T) of the photosensitizer. Moreover, sensitizers suitable for PDT, should possess *i)* a red-shifted electronic absorption band falling in the so-called therapeutic window (600-800 nm) to penetrate human tissues allowing the treatment of deeper tumours, *ii)* a high intersystem spin crossing probability and *iii)* a Δ_{S-T} higher than the energy required to generate the singlet oxygen. Other requested properties include solubility in aqueous media, redox stability, absence of intermolecular aggregation phenomena which decreases the photodynamic action and no toxicity in the dark.

There are a number of photosensitizers whose excited triplet lifetimes are too short to permit a Type-II process to occur. For this reason, much efforts are devoted to the synthesis of compounds with excited triplet state having long lifetimes. The strategy to incorporate organic chromophores into Ru(II) scaffolds attempts to accomplish this requirement. The resulting dyads systems are

characterized by the installation of an additional low-lying ^{3}IL state of organic triplet character which are able to extend the excited state lifetimes compared to traditional Ru(II) complexes that do not invoke ^{3}IL states. Pyrene chromophore has been employed so far to establish excited state equilibration between the organic ^{3}IL state and the Ru(II)-based ^{3}MLCT. [4] The energy of the organic triplet was further lowered by using spacers to link pyrene to the Ru's phenanthroline ligand, [5] achieving the longest lifetime for Ru(II) dyads to date. [6]

In view of their interesting properties, α-oligothiophenes have been recently used to obtain Ru(II) dyads with promising physico-chemical characteristics. [7,8] The in vitro PDT effect of these compounds was found to increase with the polythiophene chain length. [8] Among them, Ru(II)-polypyridyl complexes with three thiophene units (Scheme 1), has been suggested to act via a dual TypeI/II photosensitization processes, depending on the tissue oxygen tension, broadening the spectra of applicability of PDT, and it is currently under optimization for clinical phase I trials. [7,8] Moreover, it has been suggested to photocleave DNA when exposed to visible light. Both Type-I and II pathways hence, could play a pivotal role in inducing light-mediated damages to DNA.
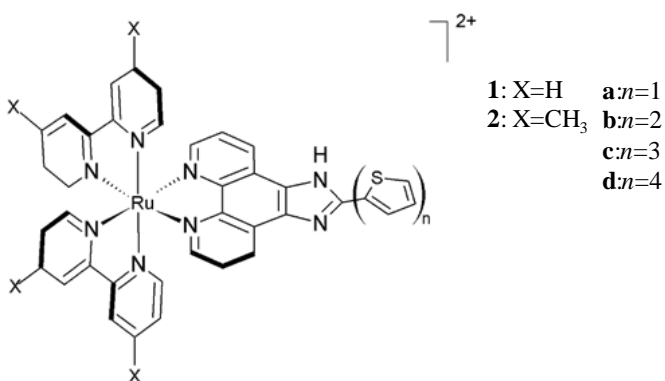
Scheme: 1 Investigated Molecules

In order to shed light on the photochemistry of these molecules, we report a careful DFT and TDDFT investigation of the photophysical properties of Ru(II) dyads containing either 2,2'-bipyridine (bpy) (**1**) or 4,4'-dimethyl-2,2'bipyridine (dmb) (**2**) as coligands, and in which polythiophene chains of different lengths (**a-b**) are incorporated at C2 of the coordinating imidazo[4,5-f][1,10]phenantroline ligand (IP) (Scheme1).

The influence of the increasing number of thiophene units on the crucial chemical and physical properties of the photosensitizer has been accurately described investigating the UV-Vis spectra, Type I and Type II photoreactions, also including spin orbit coupling values (SOC).

Results reveal that all the investigated compounds (**1a-d** and **2a-d**) possess a Δ_{S-T} gap high enough to ensure the O_2 $^3\Sigma_g^- \rightarrow ^1\Delta_g$ transition, combined with not-negligible SOC values. Nevertheless, 3 or 4 thiophene units are required to allow the installation of a low energy absorption band with an organic character, which could be useful for application in PDT. Inspection of the excited states of all the compounds, reveal that a very low-lying ^{3}IL state is afforded with the increasing of the thiophene ligands, which could be populated by ISC mechanism and can promote also Type I photoreactions, generating a reducing form of the sensitizer subsequently scavenged from oxygen leading to the superoxide anion. A fast bimolecular decay to yield oxidising species as H_2O_2 and OH· can thus, easily take place. Moreover, our results show that $O_2^{·(-)}$ can act itself as reducing agent for other Ru(II)-dyads in the triplet state, which may be one rationale for the high phototoxicity induced by these compounds even at low oxygen concentration.

2. COMPUTATIONAL DETAILS

All the calculations herein presented have been performed at DFT and its time-dependent TD-DFT formulation [9] by using the Gaussian 09 program code. [10] A preliminary benchmark study was conducted testing several exchange-correlation functionals (M06, [11] M06L, [12] M062X, [11] B3LYP, [13,14] Cam-B3LYP, [15] PBE0, [16] wB97XD [17]) against the experimental data available for molecule **1a**, [18] in methanol. The XC functionals and their performances have been evaluated comparing both calculated geometrical parameters and absorption electronic spectra with available experimental data. 6-31+G** basis set was used for all atom except for Ru one, which was described by the quasi-relativistic Stuttgart-Dresden pseudopotential. [19] Water environment was simulated by means of the integral equation formalism polarizable continuum model (IEFPCM), [20] which corresponds to a linear response in non-equilibrium solvation. Spin-orbit matrix elements were computed by using the quadratic-response TDDFT approach, [21,22] as implemented in the Dalton code, [23] at their ground-state optimized geometries, using the approximate 1-electron spin-orbit operator with scaled nuclear charges. [24] For this purpose, B3LYP was used coupled with the cc-pVDZ basis set for all atoms and SDD pseudopotential on the metal ion. Spin-orbit couplings (SOCs) have been defined according to the following formula:

$$SOC_{ij} = \sqrt{\sum_n \left| \langle \psi_{S_i} | \hat{H}_{SO} | \psi_{T_{j,n}} \rangle \right|^2}; \quad n = x, y, z$$

where $\hat{H}_{SO}$ is the spin–orbit Hamiltonian.

3. RESULTS AND DISCUSSION

3.1 Benchmark of XC Functionals and Ground State Properties

In order to select the most appropriate XC functional to accurately describe geometrical parameters and electronic transition energies for the systems under evaluation, a series of preliminary computations have been carried out testing several XC density functionals against the experimental data available for molecule **1a**, [18] in methanol (See S1 and S2). Results, collected in Table S1, show that PBE0 [16] reproduces with great accuracy the geometrical parameters and it has been chosen as the most suitable XC functional for the ground state molecular optimizations. Nevertheless, the computed absorption spectra reveal that M06[11] outperforms significantly the other XC functionals in the reproduction of the absorption spectra, and in particular at high wavelengths, although PBE0 give also good results (See S2). The computed absorption peaks for **1a** in methanol, are in good agreement with the experimental bands, as it is reported in Figure S3. Each band has been assigned on the basis of the involved molecular orbitals. The very good performances of M06 have emerged also in previous studies on metallic compounds. [25,26]

The optimized **1a-1d** structures are reported in Figure 1. The very similar structures obtained for **2a-2d** and selected geometrical parameters are reported in the SI section.
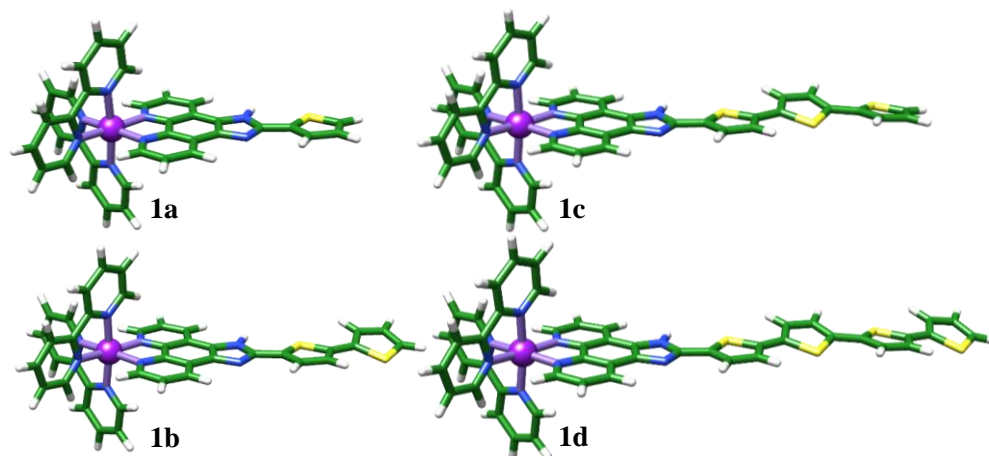
Figure: 1 Optimized **1a-1d** molecules, in the most stable conformations

The introduction of the electron-donating thiophene group onto the Ru-coordinated electron-withdrawing IP unit, extend the molecular planarity of the rigid imidazole-containing phenantroline ligand. The dihedral angles between the adjacent imidazole and thiophene ring are found to be equal to 3.5 degrees in the presence of one thiophene ligand (**1a, 2a**), and slightly varies as the chain grows, reaching the minimum value with a 4-units chain (**1d, 2d**).

The Ru(II) centre maintains its nearly ideal octahedral geometry along the **a-d** series and the sequential addition of thiophene units do not have any effect on the Ru-N distances, which keeps the same average values in all the complexes. The increasing of the chain provides more conformational flexibility and the additional thio- units (**b-d**) adopt positions which deviate from the thiophene-IP plane.

Different conformations have been tested for complexes with more than 2 thiophene units. The addition of the groups with sulphur atoms in trans between them, resulted in more stable structures, although the cis conformations lie in a range of very few kcal/mol compared with trans analogues.

Anyway, cis and trans isomers display very similar photophysical properties and the conclusion herein derived for trans compounds can be easily transferred also on cis isomers. (see S5, S6)

3.2 UV-Vis Absorption Spectra

In order to evaluate the effect of the variable number of thiophene units on the photophysical properties of Ru^{II}-dyads, the electronic absorption spectra of molecules **1a-d** and **2a-d** have been computed in water and their superposition is reported in Figure 2, together with main photophysical parameters.
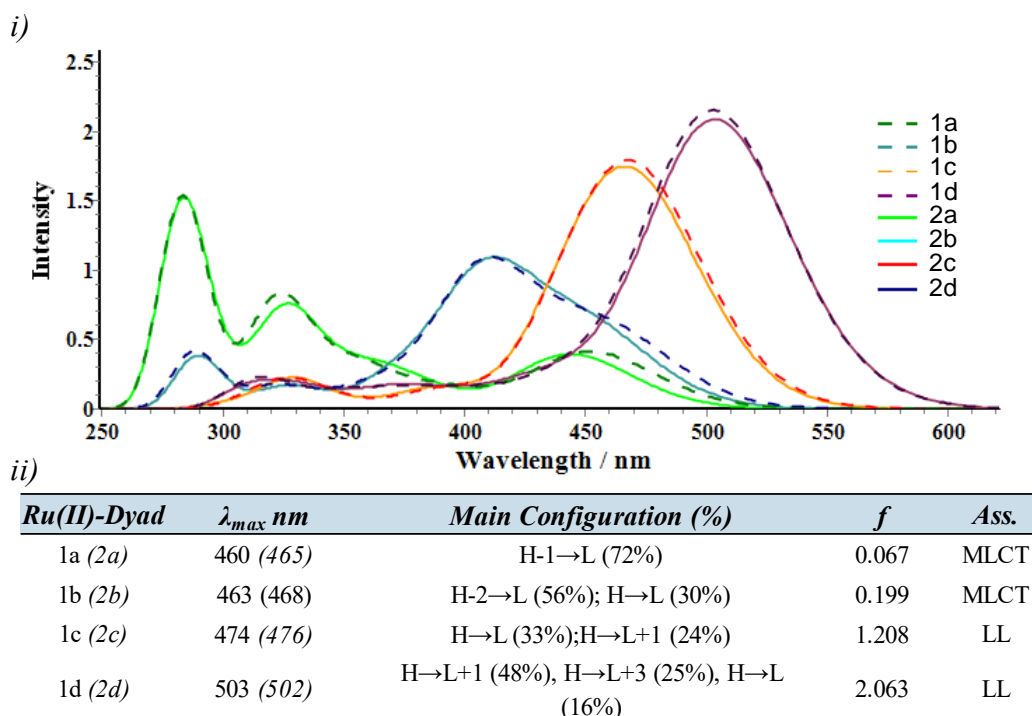

i)

ii)

Ru(II)-Dyad	λ_{max} nm	Main Configuration (%)	f	Ass.
1a *(2a)*	460 *(465)*	H-1→L (72%)	0.067	MLCT
1b *(2b)*	463 (468)	H-2→L (56%); H→L (30%)	0.199	MLCT
1c *(2c)*	474 *(476)*	H→L (33%);H→L+1 (24%)	1.208	LL
1d *(2d)*	503 *(502)*	H→L+1 (48%), H→L+3 (25%), H→L (16%)	2.063	LL

Figure 2. *i)* Computed Absorption Spectra of **1a-d** and **2a-d**, in water, at the M06/6-31+G(d,p) / SDD level of theory; *ii)* λ_{max} reported in nm, oscillator strengths, *f*, main configuration and theoretical peak assignment, for **1a-1d** (**2a-2d** in parenthesis), in water solvent; See also S3 for more details.

9

All the molecules are efficient light absorbers throughout the visible region, although significant differences can be underlined in going from **1a** and **2a** to dyads containing more than one thiophene unit. Actually, with the increasing of the delocalized π-system, a significant red shift of the λ_{max} is observed. Compounds **1a** and **2a** show the strongest bands in the UV region, computed at 282 and 330 nm in both cases, in great agreement with the experimental values available for molecule **1a**[18] (289 and 330nm). On the contrary, two weaker bands were experimentally located at higher wavelengths for **1a**, at 425 and 461 nm.[18] Actually, the computed **1a** spectrum reproduces with accuracy both of them. According to our results, the band experimentally found at 425 nm, arises from two transitions of similar intensity, computed at 439 and 443nm, while the lowest energy transition has been computed at 460nm. (See S3 for more detailed information).

On the contrary, Ru(II)-dyads with polythiophene chains show the strongest band in the visible region of the spectrum. The intensity and the position of the λ_{max} increases systematically with n, and it is a direct consequence of the reduced HOMO-LUMO gap observed as the number of thiophene increases, as reported in Figure 3. Actually, the highest-occupied molecular orbital changes in nature along the **a-d** series, being localized on the metal centre in the case of **1a** and **2a** but on the imidazo-phenantroline (IP) ligand when n=2,3 and 4. The incorporation of a polythiophene chain into Ru(II) scaffold, thus, produce the installation of an additional HOMO orbital of organic character lying at higher energies in the case of n >1, leaving the HOMO-1 orbitals at the same energy and with the same Ru(II)-based character of the **1a** and **2a** HOMO (See Figure 3 and S7). On the contrary, the LUMO orbital does not suffer any changes with the chain extension, being localized on the polypiridyl ligand in all cases (See S7, S8).

The λ_{max} is MLCT in nature in the case of **1a** and **1b** (and **2a,2b**), while neither in **1c** (**2c**) nor in **1d** (**2d**) it includes the metal contribution, being the donor and acceptor orbitals, in both cases,

localized on the ligands. This effect produces a shift of λ_{max} at high wavelengths and enables compounds with n=3 and n=4 to absorb in region above 475 nm not accessible to classical Ru(II)-polypiridyl compunds. The increasing of *n* results to be useful to move the absorption band to lower energy, changing its nature from a MLCT to a ligand-ligand one, opening interesting perspective on the use of Ru-polypiridyl polythiophene complexes (n=3,4) as candidate photosensitizers for PDT.
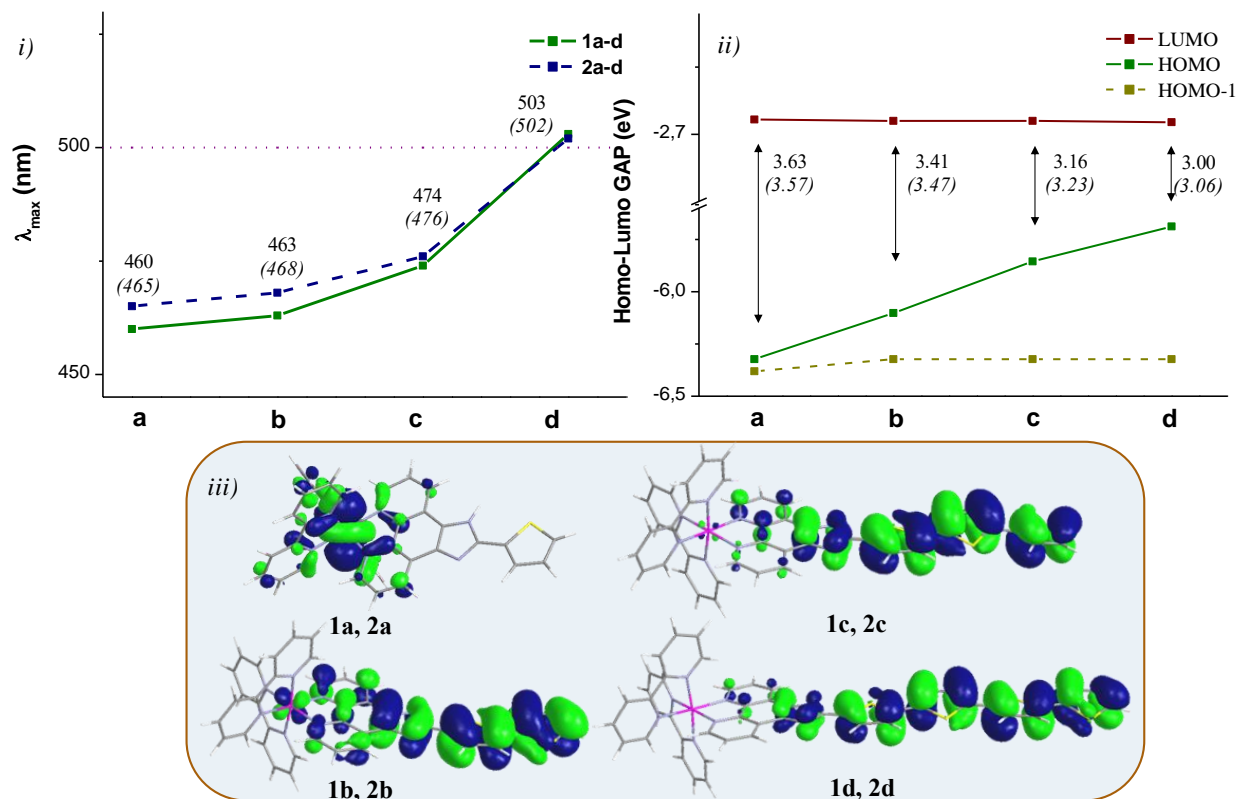

Figure 3. Plot of *i)* Maximum absorption wavelength λ_{max}, *ii)* Homo-Lumo Gap, for **1a-d** and *2a-d (in parenthesis)*; *iii)* Ru(II)-based HOMO for **1a** and **2a** and IP-based HOMOs for molecules **1b-d** and **2b-d**, at the M06/6-31+G(d,p)/SDD level of theory, in water.

3.3 Type I/II photoreactions

The ability of a sensitizer to promote Type II photoreactions depends on the efficiency of the energy transfer process between the excited triplet photosensitizer and molecular oxygen required to generate the singlet cytotoxic species $^1O_2$. To ensure the $O_2\ ^3\Sigma_g^- \rightarrow {}^1\Delta_g$ transition and to achieve a good singlet oxygen quantum yield, a PS must possess a singlet-triplet energy gap larger than that of O_2 to allow the energy transfer process to take place. Obviously, an efficient triplet state population by ISC mechanism from a singlet state is an indispensable requirement. The lowest singlet state for oxygen has been computed to be 0.90 eV, [27] in good agreement with the experimental value of 0.98 eV.

The plot of singlet-triplet energy gap (Δ_{S-T}) reported in Figure 4, shows that all compounds could promote the formation of singlet oxygen, the first triplet state of all the investigated dyads lying above the $O_2\ ^3\Sigma_g^-$ one.
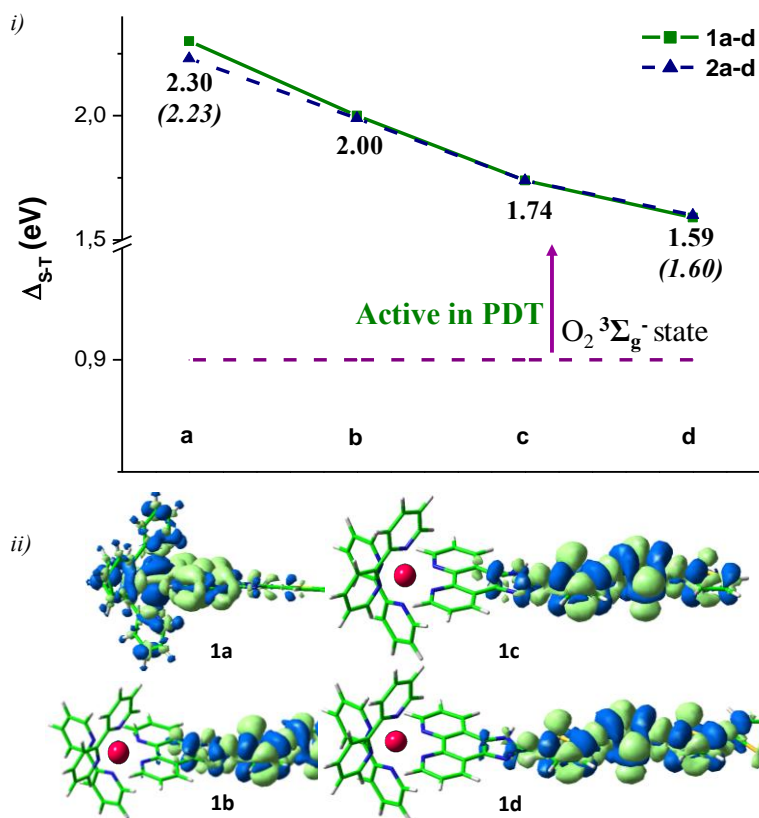
Figure 4. *i)* Singlet-triplet energy gap(Δ_{S-T}) for **1a-d** and **2a-d**, in water, at the M06/6-31+G(d,p)/SDD level of theory. If different, values relative to **2a-d** compounds are reported in italic, in parenthesis; *ii)* Electron Density Differences Plots between S_0-T_1, for **1a-1d** molecules

Interestingly, the plot reveals that the first triplet state experiences a great stabilization as a function

of *n*. Indeed, the triplet state of **1a** and **2a** dyads has been localized at 2.30 and 2.23 eV,

respectively, and reduces in energy systematically as the polythiophene chain increases, reaching

the minimum value of 1.59 and 1.60 eV for **1d** and **2d**, respectively. The observed drop in the

triplet state energy derives from the π-expansive polythiophene chromophore which confers an

organic IL character to the excited state. Actually, while the T_1 state for **1a** and **2a** is a ^{3}MLCT

state, in Ru(II)-dyads with polythiophene chains from 2 to 4 we observe the installation of low-

lying ^{3}IL states. The analysis of the electronic difference density plots between S_0 and T_1 excited

state (Figure 4*ii*), shows the involvement of Ru metal in the case of **1a** while confirm the triplet IL

nature for n≥2. It is not surprising that the triplet state energy computed for dyads with more than one thiophene unit is similar to that found for the corresponding α-oligothiophene free (See S9), confirming the increasing organic nature of the triplet state with n (i.e. 2.00 eV vs 2.31 eV for **1b** and di-thiophene (**2T**), 1.74 eV against 1.96 eV for **1c** and tri-thiophene(**3T**) and 1.59 vs 1.62 eV for **1d** and **4T**). In the case of **1a** (and **2a**) compounds, the same it is not true, being the triplet state energy of the dyad greatly stabilized with respect to that computed for the thiophene ligand free, sustaining the metal involvement in the triplet state (2.30 eV vs 3.44 eV for **1a** and thiophene, respectively). It should be recalled that the drop in ^{3}IL state energy has been connected with longer lifetimes [8] for Ru(II) dyads.

The energy diagram for the lowest S_n and T_m excited states is reported in Figure S10. A large number of triplet states lie below the first bright excited singlet one, and each one could contribute to populate the T_1 state by internal conversion, provided that an efficient intersystem spin crossing process takes place from excited singlet states. To establish the feasibility of the intersystem crossing process, spin orbit coupling values (SOC) between several excited singlet and triplet states have been computed for molecules **1a-1d** and **2a-2d**. Values are reported in table S11. The rationalization of the obtained data is not trivial but the comparison between them allow us to devise some considerations. The highest SOC values are obtained for compounds **1a** and **2a**, in which just one thiophene group is linked to the IP ligand. The most favourable channel for them involve high excited singlet and triplet states. It is noteworthy that, in the case of **1a** and **2a** molecules, the S5 is the first bright state. Actually, the highest values are found for the channels involving S5 and the lower S4 state, with triplet states very close in energy to them (T7, T8, T9 and T10). Table 1 lists the SOC values of the major ISC channels (S_n to T_m) of **1a** and **2a**, together with the S_n-T_m energy gaps. In view of the high spin-orbit values computed for them, a direct ISC

channel from S5 and S4 states to very close triplet states could be then hypothesized. SOC of comparable order of magnitude (>150 cm^{-1}) have been also recently reported for another Ru(II) compound. [26]

On the contrary, compounds containing an increasing number of thiophenes (n>2), display SOC values relatively small and equal to few tens of cm^{-1} (See S11). This result can be ascribed to the increasing organic character imparted to the occupied molecular orbitals by the polythiophene chain. Accordingly, the smallest values are those displayed by **1d** and **2d** dyads. Nevertheless, it should be recalled that values between 0.2 and 5.0 cm^{-1} are considered large enough to induce ISC on a nanosecond time scale [28] and that organic molecules approved for PDT display very small SOC values even though they are able to efficiently produce the cytotoxic singlet oxygen. [29] As a consequence, a population of triplet states can be hypothesized for all the investigated compounds.

|	**1a (2a)**				
(n,m)	**SOC(S_n-T_m)**	**ΔS_n-T_m**	**(n,m)**	**SOC(S_n-T_m)**	**ΔS_n-T_m**
4,7	229 (193)	0.14 (0.14)	5,7	354 (291)	0.20 (0.17)
4,8	306 (43)	0.14 (0.06)	5,8	283 (41)	0.17 (0.09)
4,9	47 (311)	0.04 (0.00)	5,9	46 (204)	0.07 (007)
4,10	345 (56)	0.02 (-0.02)	5,10	168 (158)	0.05 (0.05)

Table 1. SOC values (cm^{-1}) and singlet-triplet energy gap **ΔS_n-T_m** (eV) for the major ISC channels involving S_n (n=4,5) and T_m (m=7,8,9,10) states, for **1a** and **(2a)** molecules.

The populated excited triplet state could also follow a different deactivation pathway photogenerating the superoxide anion $O_2^{\cdot-}$ and ROS, instead of transfer its energy to produce the singlet oxygen species. For **1c** and **2c** dyads it was previously suggested the possibility to switch to a type I mechanism mediating photoinduced electron transfer reactions. [8] The feasibility of such kinds of photoreactions, can be established computing the vertical electron affinity (VEA)

and ionization potentials (VIP) for each molecule and molecular oxygen. [30] Results are listed in Table2.

Type I reactions involves electron or hydrogen-atom transfer between the excited sensitizer (usually T_1) and substrate molecules, such as the cell membrane or the sensitizer itself, to yield radical ions and free radicals. These radicals can then interact with oxygen to produce oxygenated products. Different pathways can be followed to generate O_2^- species which then undergo fast bimolecular decay to yield oxidizing species as H_2O_2 and $OH^\cdot$, able to promote reactions with biomolecules. [2]

The superoxide anion $O_2^{\cdot(-)}$ can be produced by direct electron transfer from the photosensitizer to molecular oxygen according to reaction *(I)*:

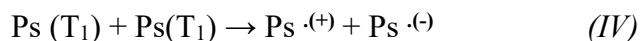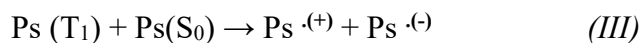$$Ps\ (S_0) + {}^3O_2 \rightarrow Ps^{\cdot(+)} + O_2^{\cdot(-)} \qquad (I)$$
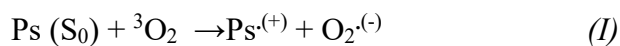
Such reaction is still of Type II-oxygen reactions and result to be less feasible as the thiophene chain grows. With the increasing of n indeed, the triplet state become weaker electron donors and it is not able to promote the direct electron transfer in water. According to our data, only in the case of **2a** the process is, to some extent, likely to occur, being the sum of VIP(T_1) and the electron affinity of ${}^3O_2$ (-3.43 eV at the same level of theory), slightly negative.

An alternative pathway to generate $O_2^{\cdot(-)}$ may proceed through electron transfer from the reduced form of dyads to molecular oxygen, provided that the summation of the electron affinity of ${}^3O_2$ and VEA PS (S_0/T_1) is negative:

$$Ps^{\cdot(-)} + {}^3O_2 \rightarrow {}^1Ps + O_2^{\cdot(-)} \qquad (II)$$

16
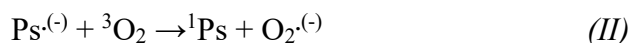
The Ps$^{\cdot(-)}$ species could be formed in solution in presence of electron donors in the near vicinity e.g. a DNA base, or through the so-called autoionization reactions *(III* and *IV)* which imply the reduction of T_1 state of Ps by neighbouring S_0 or T_1 state of Ps itself (Type-I photoreactions):

$$Ps\ (T_1) + Ps(S_0) \rightarrow Ps\ ^{\cdot(+)} + Ps\ ^{\cdot(-)} \qquad\qquad \textit{(III)}$$

$$Ps\ (T_1) + Ps(T_1) \rightarrow Ps\ ^{\cdot(+)} + Ps\ ^{\cdot(-)} \qquad\qquad \textit{(IV)}$$

According to our results, the T_1 states of all the compounds can be reduced through autoionization reactions by neighbouring T_1 ones, the sum of VEA (T_1) and VIP (T_1) being negative. More interestingly, all the reduced dyads can transfer an electron to the molecular oxygen in its ground state through reaction *(II)* producing the superoxide anion, as confirmed by the higher electron affinity of oxygen if compared with that of the sensitizer. Moreover, the superoxide anion can act itself as reducing agent for dyads in the triplet state, which maybe one rationale for the fact that the phototoxicity induced by these compounds is high even at low oxygen concentration.

	1a *(2a)*	1b *(2b)*	1c *(2c)*	1d *(2d)*
VEA	-2.87*(-2.81)*	-2.88*(-2.82)*	-2.88*(-2.82)*	-2.88*(-2.82)*
VIP	5.94 *(5.61)*	5.72*(5.71)*	5.48*(5.48)*	5.33*(5.33)*
VEA(T_1)	-4.90*(-5.04)*	-4.88*(-4.82)*	-4.62*(-4.56)*	-4.47*(-4.42)*
VIP (T_1)	3.64 *(3.38)*	3.72*(3.71)*	3.74*(3.74)*	3.74*(3.73)*

Table 2: VEA and VIP values (eV) in water, for $^3O_2$ molecule and for **1a-1d** and **2a-2d** Ru(II)-dyads in their singlet and triplet states, computed at PBE0/ 6-31+G**/SDD. The O_2 electron affinity (-3.42 eV) has been computed at the same level of theory.

Based on our results, all the investigated dyads can undergo Type I photoreactions. Nevertheless, only compounds containing 3 and 4 thiophene ligands display a low energy absorption band to be useful in PDT through type II mechanism. They are, accordingly, able to afford a low-lying ^{3}IL

states which can contribute to the dual TypeI/II photoreactivity, and exert their phototoxicity at different oxygen tension.

Conclusions

A careful DFT and TDDFT investigation has been carried out on very promising Ru(II) dyads incorporating polythiophene chains of different lengths. The influence of the increasing number of thiophene units ($1 \leq n \leq 4$) on the crucial chemical and physical properties of the photosensitizer, has been accurately described investigating the UV-Vis spectra, Type I and Type II photoreactions, also including spin orbit coupling values (SOC).

Results reveal that the incorporation of a polythiophene chain into Ru(II) scaffold produces the installation of an additional HOMO orbital of organic character lying at higher energies in the case of $n > 1$, shifting the λ_{max} towards higher wavelengths and enabling compounds with n=3 and n=4 to absorb in region above 475 nm not accessible to classical Ru(II)-polypiridyl compunds. The organic chromophore produces a change of the absorption band which acquires an increased ^{1}LL nature as the chain grows. More importantly, results reveal that the increasing of the π-expansive polythiophene chromophore confers an organic IL character to the first triplet excited state producing a systematic drop in its energy. The first triplet state changes from being a ^{3}MLCT to a pure ^{3}IL state when n=3 and 4. In all cases, the $\Delta_{\text{S-T}}$ gap is high enough to ensure the $O_2\ ^3\Sigma_g^- \rightarrow ^1\Delta_g$ transition combined with not-negligible SOC values which indicate an efficient triplet population by ISC mechanism. The magnitude of SOC values are inversely proportional to the chain length and decrease with the increasing of the organic character of the involved states. The high activity experimentally found for compound **1c** can be then ascribed to the efficient energy transfer from

the stable ^{3}IL state to oxygen, accessible by ISC mechanism after irradiation with a low energy source. Same conclusion can be extended to **2c**, **1d** and **2d** compounds.

Results show that the populated triplet states can undergo also Type I photoreactions, generating a reducing form of the sensitizer subsequently scavenged from oxygen leading to the superoxide anion. A fast bimolecular decay to yield oxidising species as H_2O_2 and $OH\cdot$ can thus, easily take place in all cases. Moreover, our results show that $O_2^{\cdot(-)}$ can act itself as reducing agent for other Ru(II)-dyads in the triplet state, which may be one rationale for the high phototoxicity induced by these compounds even at low oxygen concentration.

ASSOCIATED CONTENT

Supporting Information. Selected geometrical parameters of optimized molecules (1a-d and 2a-2d), detailed computed UV-Vis Spectra, Molecular Orbitals Plots, Diagram of S_n and T_n vertical excitation states, energy and SOC values for **1a-1d** and **2a-2d**. Additional data on less stable conformers. "This material is available free of charge via the Internet at http://pubs.acs.org."

AUTHOR INFORMATION

Corresponding Author

*Marta Erminia Alberto, *E-mail: marta.alberto@chimie-paristech.fr*

REFERENCES

1. Padilla, R.; Rodriguez-Corrales, J.A.; Donohoe, L.E.; Winkel, B. S. J.; Brewer, K.J. *Chem. Commun.* **2016**, *52,* 2705-2708; b) Wachter, E.; Heidary, K.; Howerton, B. S.; Parkin, S.; Glazer, E. C. *Chem. Commun.* **2012**, *48*, 9649-9651; c) Mari, C.; Pierroz, V.; Ferrari, S.; Gasser, G. *Chem. Sci.*, **2015**, *6,* 2660-2686; d) Farrer, N.J.; Salassa, L.; Sadler, P. J. *Dalton Trans.*, **2009**, 10690-10701; e) Liu, Y.; Hammitt, R.; Lutterman, D. A.; Joyce, L.E.; Thummel, R.P.; Turro, C. *Inorg. Chem.* **2009**, *48*, 375-385;

2. Quirk, B.J.; Brandal, G.; Donlon, S.; Vera, J.C.; Mang, T. S.; Foy, A.B.; Lew, S.M.; Girotti, A. W.; Jogal, S.; LaViolette, P.S.; Connelly, J.M.; Whelan, H.T. *Photodiagn Photodyn Ther* **2015**, *12*, 530-544; b) Dolmans, D.E.J.G.J.; Fukumura, D.; Jain, R.K. *Nature Rev. Cancer*, **2003**, *3,* 380-387; c) Yano, S.; Hirohara, S.; Obata, M.; Haguya, Y.; Ogura, S-I.; Ikeda, A.; Kataoka, H.; Tanaka, M.; Joh, T. *J. Photochem. Photobiol. C*, **2011**, *12,* 46-67; d) Castano, A. P.; Mroz P.; Hamblin, M. R. *Nat. Rev. Cancer*, **2006**, *6*, 535-545; e) Castano, A. P.; Demidova, T. N.; Hamblin, M.R. *Photodiagnosis and Photodyn Ther.* **2004**, *1*, 279-293;

3. Lang, K.; Mosinger, J.; Wagnerová D. M. *Coord. Chem.Rev*, **2004**, *248*, 321-350; b) DeRosa, M.C; Crutchley R.J *Coord. Chem. Rev.* **2002**, *233-234,* 351-371;

4. a) McClenaghan, N.D.; Leydet, Y.; Maubert, B.; Indelli, M.T.; Campagna, S. *Coord.Chem. Rev.* **2005**, *249*, 1336-1350; b) Reichardt, C.; Pinto, M.; Wächtler, M.; Stephenson, M.; Kupfer, S.; Sainuddin, T.; Guthmuller, J.; McFarland, S.A.; Dietzek B. *J. Phys. Chem. A* **2015***, 119*, 3986-3994;

5. Monro, S.; Scott, J.; Chouai, A.; Lincoln, R.; Zong, R.; Thummel, R.P.; McFarland, S.A. *Inorg. Chem.* **2010**, *49*, 2889-2900;

6. Lincoln, R.; Kohler, L.; Monro, S.; Yin, H.; Stephenson, M.; Zong, R.; Chouai, A.; Dorsey, C.; Hennigar, R.; Thummel, R.P.; McFarland, S.A. *J. Am. Chem. Soc.* **2013**, *135,* 17161-17175;

7. a) McFarland, S.A. Metal-based Thiophene Photodynamic Compounds and Their Use. US provisional patent #61624391 filed April 15, 2012, PCT/US13/36595filed April 15, **2013**; b) http://theralase.com/pressrelease/theralase-files-us-patent-applicationincreased-targeting-photo-dynamic-therapy/.

8. Shi, G.; Monro, S.; Hennigar, R.; Colpitts, J.; Fong, J.; Kasimova, K.; Yin, H.; DeCoste, R.; Spencer, C.; Chamberlain, L.; Mandel, A.; Lilge, L.; McFarland, S.A. *Coord.Chem Rev.,* **2015**, *282-283*, 127; b) Arenas, Y.; Monro, S.; Shi, G.; Mandel, A.; McFarland S.; Lilge, L. *Photodiagn. Photodyn. Ther.*, **2013**, *10,* 615-625; c) Kaspler, P.; Lazic, S.; Forward, S.; Arenas, Y.; Mandel, A.; Lilge, L. *Photochem. Photobiol. Sci.,* **2016**, *15,* 481-495.

9. Casida M.E. In Recent Developments and Applications in Density-Functional Theory; J. M. Seminario, Eds.; Elsevier: Amsterdam, The Netherlands, 1996, 155-192.

10. Gaussian 09, Revision **E.01**, Frisch, M. J.; Trucks, G. W.; Schlegel, H. B.; Scuseria, G. E.; Robb, M. A.; Cheeseman, J. R.; Scalmani, G.; Barone, V.; Mennucci, B.; Petersson, G. A.; Nakatsuji, H.; Caricato, M.; Li, X.; Hratchian, H. P.; Izmaylov, A. F.; Bloino, J.; Zheng, G.; Sonnenberg, J. L.; Hada, M.; Ehara, M.; Toyota, K.; Fukuda, R.; Hasegawa, J.; Ishida, M.; Nakajima, T.; Honda, Y.; Kitao, O.; Nakai, H.; Vreven, T.; Montgomery, J. A., Jr.; Peralta, J. E.; Ogliaro, F.; Bearpark, M.; Heyd, J. J.; Brothers, E.; Kudin, K. N.; Staroverov, V. N.; Kobayashi, R.; Normand, J.; Raghavachari, K.; Rendell, A.; Burant, J. C.; Iyengar, S. S.; Tomasi, J.; Cossi, M.; Rega, N.; Millam, J. M.; Klene, M.; Knox, J. E.; Cross, J. B.; Bakken, V.; Adamo, C.; Jaramillo, J.; Gomperts, R.; Stratmann, R. E.; Yazyev, O.; Austin, A. J.; Cammi, R.; Pomelli, C.; Ochterski, J. W.; Martin, R. L.; Morokuma, K.; Zakrzewski, V. G.; Voth, G. A.; Salvador, P.; Dannenberg, J. J.; Dapprich,

S.; Daniels, A. D.; Farkas, Ö.; Foresman, J. B.; Ortiz, J. V.; Cioslowski, J.; Fox, D. J. Gaussian, Inc., Wallingford CT, 2009.

11. Zhao, Y.; Truhlar, D. G. *Theor. Chem. Acc.*, **2008**, *120,* 215-241.

12. Zhao, Y.; Truhlar, D. G. *J. Chem. Phys.*, **2006**, *125*, 194101: 1-18.

13. Becke, D. *J. Chem. Phys*., **1993,** *98*, 5648–5652.

14. Lee, C.; Yang, W.; Parr, R.G. *Phys. Rev. B*, **1988**, *37*, 785-789.

15. Yanai, T.; D. Tew, N. Handy, *Chem. Phys. Lett.*, **2004**, *393*, 51-57

16. Adamo, C.; Barone, V. *J. Chem. Phys.*, **1999**, *110*, 6158-6169.

17. Chai, J.-D.; Head-Gordon, M. *Phys. Chem. Chem. Phys.*, **2008**, *10*, 6615-6620.

18. Xu, F.; Peng, Y-X.; Hu, B.; Tao, T.; Huang, W. *CrystEngComm*, **2012**, *14,* 8023–8032

19. Andrae, D.; Haussermann, U.; Dolg, M.; Stoll, H.; Preuss, H. *Theor. Chim. Acta* **1990***, 77,* 123-141

20. Cossi, M.; Barone, V. *J Chem Phys* **2000**, *112*, 2427-35; b) Tomasi, J.; Menucci, B.; Cammi, R. Chem Rev **2005**, *105,* 2999-3094.

21. Rinkevicius, Z.; Tunell, I.; Sałek, P.; Vahtras, O.; Ågren, H. *J. Chem. Phys.* **2003***, 119,* 34−46.

22. Ågren, H.; Vahtras, O.; Minaev, B. Adv. Quantum Chem. **1996***, 27*, 71−162.

23. DALTON. A molecular electronic structure program. Release Dalton 2011. http://daltonprogram.org/.

24. Koseki, S.; Schmidt, M. W.; Gordon. M. S. J. Phys. Chem. A, **1998**, *102,* 10430-10435

25. Latouche, C.; Skouteris, D.; Palazzetti, F.; Barone V. *J.* Chem. Theory Comput., **2015**, *11,* 3281-3289;

26. Alberto, M.E.; Russo, N.; Adamo, C. *Chem. Eur. J.*, **2016**, *22*, 9162-9168

27. Alberto, M.E.; De Simone, B.C.; Mazzone, G.; Sicilia, E.; Russo, N. *Phys Chem Chem Phys* **2015**, *17*, 23595-23601;

28. Klessinger, M. In *Theoretical and Computational Chemistry*, Cyril, P., Ed. Elsevier: 1998, *5*, 581-610.

29. Alberto, M.E.; Marino, T.; Quartarolo, A.D.; Russo, N. *Phys.Chem.Chem. Phys.* **2013**, *15,* 16167-16171;

30. Llano, J.; Raber, J.; Eriksson, L.A. *J Photochem Photobiol A Chem.,* 2003, **154**, 235-243

"For Table of Contents Only"
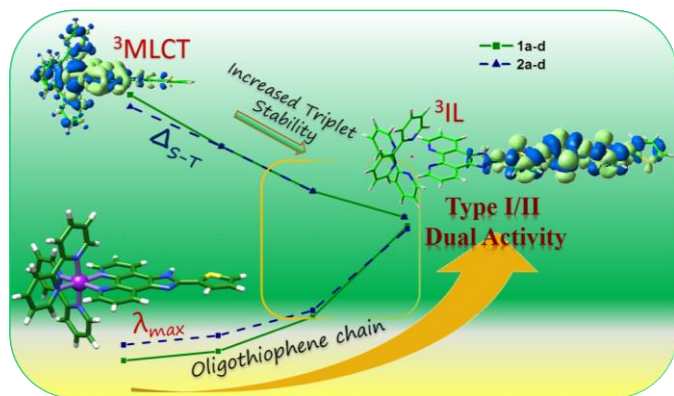
A DFT and TDDFT investigation has been carried out on very promising Ru(II) dyads of interest as anticancer agents. The modulation of the photophysical properties with the increasing of thiophene units ($1 \leq n \leq 4$) has been accurately described. The shift of the λ_{max} towards high wavelengths and the systematic drop in energy of the first triplet state as the π-expansive chromophore increases, contribute to the Type I/II dual activity of the dyads incorporating long polythiophene chains.